

Characterization and Investigation of In-Vitro Corrosion Behavior of Plasma Sprayed Hydroxyapatite and Hydroxyapatite–Calcium Phosphate Coatings on AISI 304

Gurpreet Singh ^a, Hazoor Singh ^b, and Buta Singh Sidhu ^c

^a *Mechanical Engineering Department, Punjabi University Patiala, Punjab, India,*
gurpreetsnabha@yahoo.com

^b *Yadavindra College of Engineering, Punjabi University G.K. Campus, Talwandi Sabo, Punjab, India,*

^c *Punjab Technical University, Jalandhar, Punjab, India,*

Abstract

The main aim of this study is to investigate the corrosion behavior of uncoated, plasma sprayed hydroxyapatite (HA) and hydroxyapatite–Calcium Phosphate (CaP) coated AISI 304 specimen in simulated body fluid (SBF). In HA–CaP coating 10 wt% CaP was mixed with HA. The coatings was characterized by x-ray diffraction (XRD), scanning electron microscopy (SEM) and energy dispersive X-ray spectroscopy (EDS) to investigate the crystallinity, microstructure and morphology. Electrochemical potentiodynamic tests were performed to determine the corrosion resistance of uncoated substrate and the coatings. After the electrochemical corrosion testing the exposed samples were examined by XRD, SEM and EDS. The result of electrochemical study reveals improvement in corrosion resistance of AISI 304 after HA coating.

Keywords: Plasma deposition, Coatings, Electrochemical technique, corrosion.

Introduction

Biomaterials when placed inside the human body are called bio-implants. Biocompatibility is the first and leading requirement for the selection of the biomaterial so that it should not cause any adverse reaction in the body like allergy, inflammation and toxicity either immediately after surgery or under post operative conditions [1]. Secondly, biomaterials should possess adequate mechanical strength and high fracture toughness in order to sustain the forces of high load bearing bones without failure [2, 3]. Third and most important consideration is that a bioimplant should have very high corrosion resistance, because corrosion can adversely affect the biocompatibility as well as the mechanical

properties of the implant [4]. Biomaterials are classified as ceramics, polymers, metals and alloys. Ceramic may exhibits good bio-compatibility with human body but has poor mechanical properties. Polymers are soft materials and cannot used for load bearing applications. Metals and alloys posses good mechanical properties but exhibits poor biocompatibility with human body. The literature reported that almost all metals and alloys release metallic ions which may be very toxic to human body and cause poor fixation of implants that some time leads to the implant failure [5–8].

The reaction between body fluid and implant material can be minimized by using hydroxyapatite $[(Ca_{10}(PO_4)_6(OH)_2, HA)]$ and calcium phosphate $[Ca_3(PO_4)_2, CaP]$ coatings. These coatings promote the bone healing leading to the rapid biological fixation of implants [9– 12]. Because the chemical composition of HA is similar to that of the natural bone so it exhibits outstanding osteoconduction properties in comparison to other bioactive materials [13–16].

Many commercial methods are used to deposit HA on metal implants such as dip coating–sintering [17, 18], Hot Isostatic Pressing (HIP) [19], electrophoretic deposition [20], ion–beam sputtering coating [21, 22], biomimetic deposition [23, 24], thermal spray techniques such as Atmospheric Plasma Spraying (APS) [25], Vacuum Plasma Spraying (VPS) [26] and High–Velocity Oxy–Fuel spraying (HVOF) [27]. Plasma spray is one of the most commercially viable technique to economically coat HA on implants, because of its simplicity, high deposition rates and low substrate temperature etc. [28].

In this work, the corrosion resistance of HA and HA–CaP coatings has been investigated using electrochemical corrosion testing technique. Plasma Sprayed was employed to spray HA and HA–CaP coatings on AISI 304 stainless steel substrate. The crystallinity and morphology of the coated samples before and after the electrochemical corrosion testing were analysed by XRD and SEM/EDS techniques.

Experimental Procedure

Materials

Medical grade HA and CaP powders (IFGL Bio Ceramics Limited, Kolkata, India) with particle distribution of 57 – 200 μm and 90–300 μm respectively were used as feedstock powders. AISI 304 substrates of size 15 x 15 x 3 mm were plasma sprayed with HA and HA–CaP powders. Before spraying the substrate surface was grit blasted with alumina of particle size 50 – 60 μm at a pressure of 5 bars for 2 minutes to roughen the surface and

subsequently air blasted to remove any residual grit. Because a highly roughened substrate surface exhibits higher bond strength as compared to a smooth substrate surface [29].

Development of coatings

The mixture of HA + 10 wt% CaP was prepared by mechanically stirring the powder in a ceramic pot for 20 min. The HA and HA + 10 wt% CaP coatings were deposited on AISI 304 using plasma spray (Miller Spray System) at Anod plasma Kanpur. The addition CaP in HA improves the healing rate because it improves the growth of apatite tissues. On the other side the corrosion resistance of titanium has been reduced by adding more than 10% CaP in HA [30]. So literature suggest to add 10% CaP in HA in order to maintain the balance in between the corrosion resistance and healing rate of implant in human body. The spraying parameters for both the powder were same and are listed in Table I.

Table I. Spraying Parameters for HA and HA + 10 wt% CaP Coatings

Spraying Parameter	Value
Arc Current	500 [Amp]
Arc Voltage	50 [V]
Carrier Gas (Argon) Flow Rate	5 [slpm]
Secondary Gas (Hydrogen) Flow Rate	12 [slpm]
Spraying Distance	75 [mm]
Powder Flow Rate	20–25 [g/min]

Characterization of coatings

The as-sprayed coatings were analyzed by XPERT-PRO Xray diffractometer system. In the phase analysis, the radiation source was Cu K α ; the operating generator setting was 45 kV / 40 mA. The coated samples were scanned over the 2 θ range of 20 $^{\circ}$ to 60 $^{\circ}$. The crystallite size (τ) of the coated samples before and after corrosion testing in Ringer's solution has been calculated using Scherrer's equation [31]:

$$\tau = (K \cdot \lambda) / W \cdot \cos(\theta) \quad \text{Eq. (1)}$$

where: K is dimensionless shape factor dependent on crystallite shape, $0.8 < K < 1.1$; $K = 0.94$ for FWHM (full width at half max) of spherical crystals with cubic symmetry; λ is the x-ray wavelength of monochromatic radiation ($\lambda_{\alpha 1} = 1.5405 \text{ \AA}$). W is defined as the full width of peak from the intensity distribution pattern measured at half of the maximum intensity value. θ is the Bragg angle, in degree.

Microstructural investigation was carried out on the surfaces and polished cross-sections of the coatings by SEM (EVO MA 15 ZEISS) coupled with EDX. As-sprayed coatings were cut with a low speed precision saw and mounted in hot resin using a hot mounting press, followed by polishing with emery papers of 220, 320, 400, 600, 800, 1000 and 2000 grades, and finally mirror finished by buffing using an alumina slurry solution on napped cloth. To achieve the desired conductivity for observation in SEM the gold sputter coating were applied to samples using JEOL JFC-1600 auto fine coater. Elemental analysis of the coatings was carried out using an EDX. EDX analysis was used to provide evidence of the presence of coating particles and to display the distribution of elements in the coatings as well as to evaluate Ca/P ratios of the HA and HA-CaP coatings.

Surface roughness

The surface roughness values of uncoated AISI 304, HA and both the coated specimen were measured by a roughness tester (SJ-201 MITUTOYO), using a filter of Gaussian type for a cut-off wavelength of 0.8 mm. Roughness parameters such as R_a (the arithmetic mean of the departures of the roughness profile from the mean line) was measured at different five positions on the surface of the samples. The average value of each parameter at various positions was reported here.

Electrochemical Corrosion Studies

Potentiodynamic polarization tests were conducted to investigate the electrochemical corrosion behavior of the uncoated and coated AISI 304 specimens.

Potentiostat/Galvanostat (Series G-750; Gamry Instruments, Inc. USA), interfaced with a computer and loaded with Gamry electrochemical software DC105 was used to conduct the corrosion test. Ringer's solution (Nice Chemical Pvt. Ltd. Cochin, India) with chemical composition (in g/L) as 9 NaCl, 0.24 CaCl₂, 0.43 KCl and 0.2 NaHCO₃ at pH 7.2 was used as the electrolyte for simulating human body fluid conditions. Before conducting the corrosion studies, each specimen was immersed in Ringer's solution for 24 hours for stabilization. During the in vitro potentiodynamic corrosion tests the exposed area of the samples in the Ringer's solution was 1 cm². The AISI 304 specimen forms the working

electrode. The saturated calomel electrode (SCE) was the reference electrode. A graphite rod served as the counter electrode. The instrument measures and controls the potential difference between a non-current carrying reference electrode and one of the two current carrying electrodes (the working electrode). All tests were performed at a scan rate of 1 mV/sec and fresh solution was used for each experiment. Polarization curves were initiated at -250 mV to +250 mV relative to open circuit potential.

Results and discussions

Coating Crystallinity

The XRD pattern of HA and HA + 10 wt% CaP coatings on AISI 304 are shown in Figure 1. The XRD peaks of HA + 10 wt% CaP coatings appears more sharp and has higher intensity count. According to the Scherrer's equation calculation the average crystallite size of HA and HA + 10 wt% CaP coating are 19.92 nm and 20.792 nm.

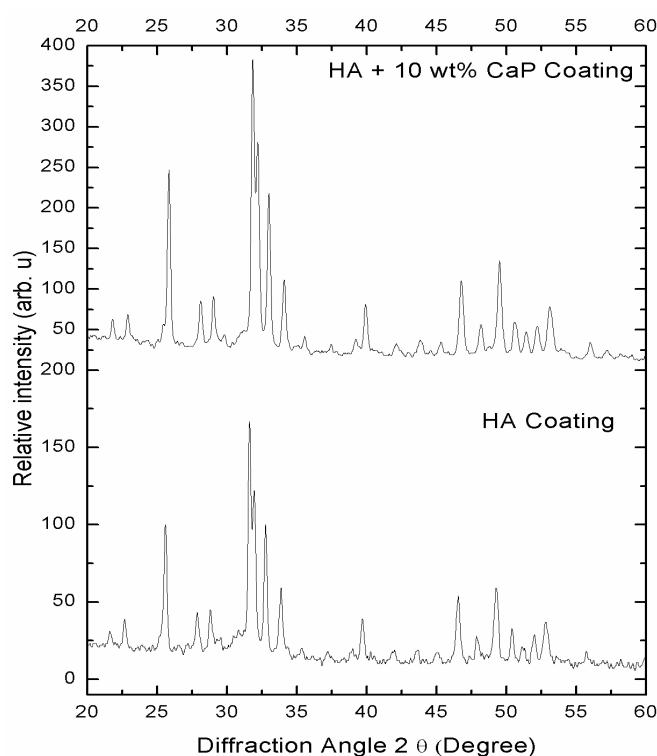


Figure 1. X-ray diffraction pattern of HA and HA + 10 wt% CaP coating on AISI 304

SEM / EDX analysis

Surface Analysis

The HA powder has the spherical shape particles whereas the CaP powder has irregular and angular shape particles. The SEM micrographs of both the feedstock powders were published elsewhere [30]. SEM micrograph of plasma spray HA coating (Figure 2 (a)) shows the microstructure consist of molten HA particles and few un-melted HA particles appear. The EDX analysis shows the presence of Ca, P and O, which are main components of HA powder at three different positions. The SEM micrograph of HA + 10 wt% CaP coating surfaces (Figure 2 (b)) shows that microstructure consist of pores / voids and unsmooth. It is generally believed that if the density of coating surface is higher than the corrosion resistance of the surface increase. The average value of Ca/P ratio of the HA and HA + 10 wt% CaP coating are 1.6 and 1.7 respectively which lies in between the guidelines described by the Food and Drug Administration and in the ISO standards [32, 33].

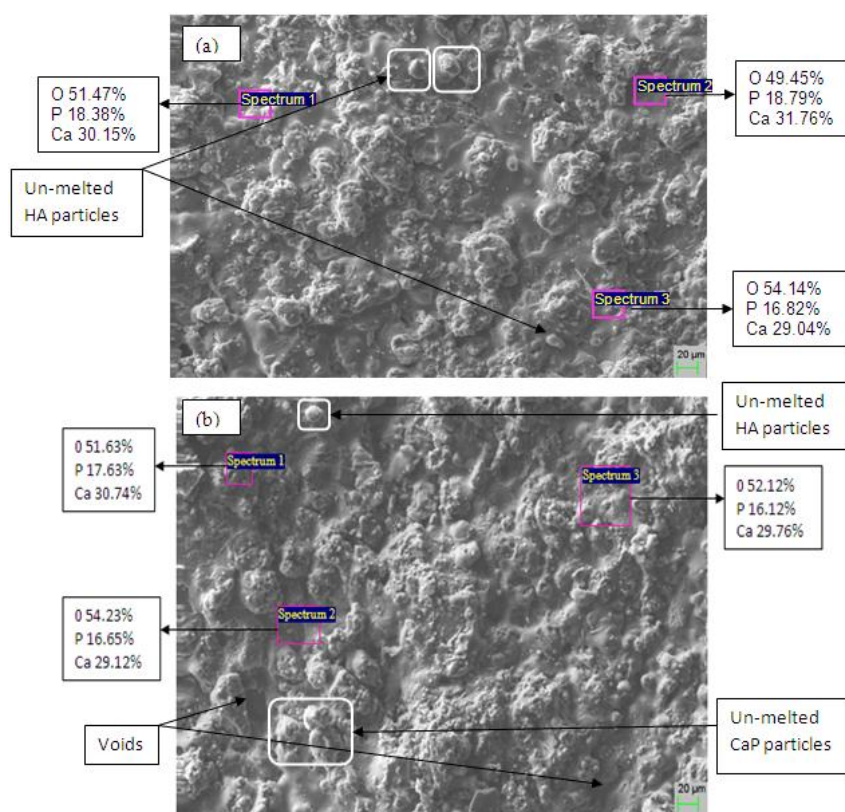


Figure 2. SEM micrograph and EDX analysis of plasma sprayed (a) HA coating (b) HA + 10 wt% CaP coating on AISI 304

Cross-Sectional analysis

The morphology of the plasma sprayed HA and HA + 10 wt% CaP coatings on AISI 304 at the cross-section is investigated by SEM and EDX and is shown in Figure 3. The thickness of coatings was measured at four positions and the average thickness was $100 \pm 20 \mu\text{m}$. The increase in proportion of CaP promotes the osteoconduction while HA particles carry the biological apatite precipitation [34]. It has been reported in literature that high soluble coating are more osteoconductive and bioactive in comparison to the stable layers in-vivo [35]. The osteointegration of CaP coatings is faster than HA coatings in non – load bearing conditions [36].

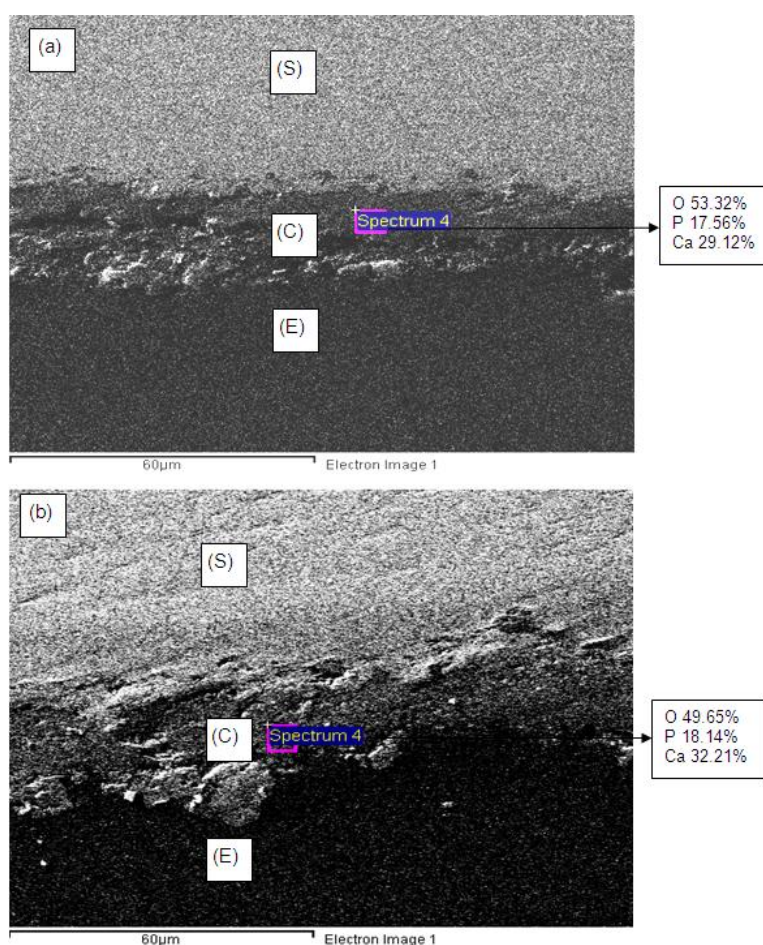


Figure 3. SEM and EDX along the cross-section of plasma sprayed (a) HA coating (b) HA + 10 wt% CaP coating on AISI 304 (S, C, E, represents the substrate, coating and epoxy respectively)

Surface roughness

Surface roughness of implant plays a vital role in tissue interaction and also affects the biocompatibility in clinical use. Higher surface roughness facilitates the cell growth. The results of average surface roughness value (R_a) of all plasma coating on AISI 304 demonstrate that surface roughness value HA coated AISI 304 ($5.884 \pm 0.3 \mu\text{m}$) is less than HA + 10 wt% CaP coated AISI 304 ($7.012 \pm 0.3 \mu\text{m}$). The increase in the surface roughness may be because of larger particle size of reinforced CaP.

Electrochemical Corrosion testing

The potentiodynamic scan of the uncoated, plasma sprayed coatings on AISI 304 samples in Ringer's solution is shown in Figure 4. The corrosion parameters such as anodic tafel slope (β_a), cathodic tafel slope (β_c), corrosion potential (E_{Corr}), and corrosion current density (I_{Corr}) are determined from the potentiodynamic curves by conducting the Tafel extrapolation test.

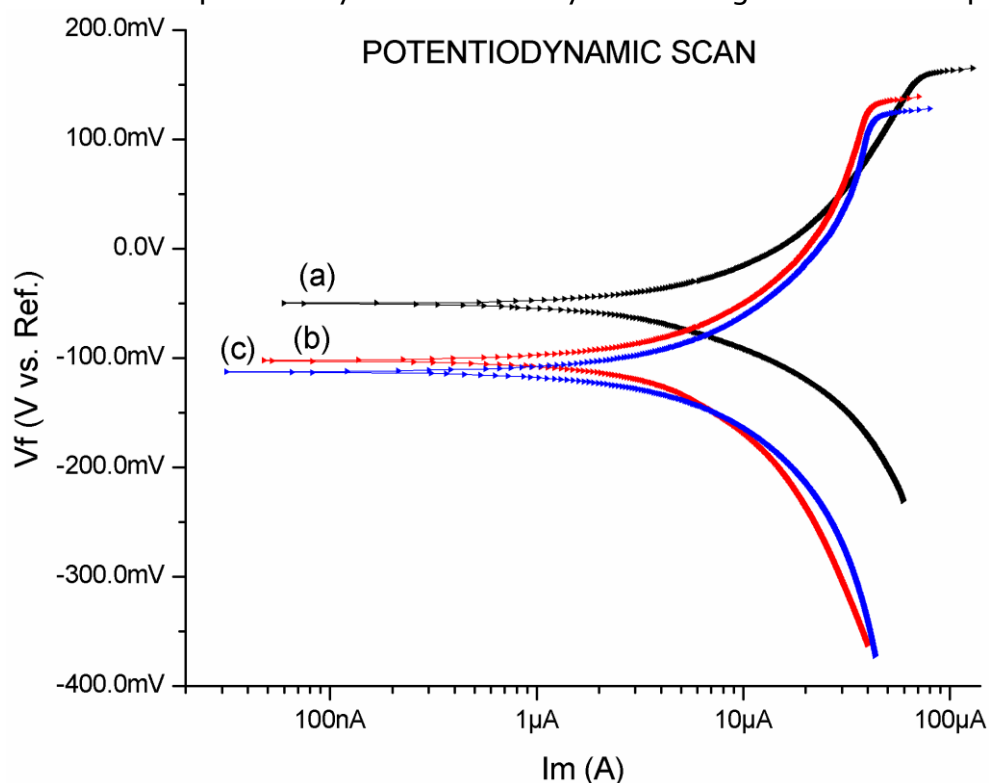


Figure 4. Potentiodynamic curves of (a) uncoated (b) HA coating (c) HA + 10 wt% CaP coating on AISI 304 in Ringer's solution

The results of these corrosion parameters are shown in Table II. The chance of corrosion in a material depends upon the corrosion current density (I_{Corr}) at a given potential, material will be more corrosion resistant at lower value of I_{Corr} [37–39].

Table II. Corrosion parameters determined by the Tafel extrapolation test

Parameter	Uncoated	HA Coated	HA + 10 wt% CaP Coated
β_a [e-3 V/decade]	136.0	177.0	125.1
β_c [e-3 V/decade]	385.6	351.3	136.2
E_{Corr} [mV]	-50.10	-102.0	-113.0
I_{Corr} [μA]	3.72	1.95	2.11

The result of Tafel slope values shows that corrosion current density of uncoated sample in Ringer's solution is ($I_{\text{Corr}} = 3.72 \mu\text{A}$, $E_{\text{Corr}} = -50.10 \text{ mV}$) higher than the plasma sprayed HA ($I_{\text{Corr}} = 1.95 \mu\text{A}$, $E_{\text{Corr}} = -102 \text{ mV}$) and HA + 10 wt% CaP ($I_{\text{Corr}} = 2.11 \mu\text{A}$, $E_{\text{Corr}} = -113.0 \text{ mV}$) coated AISI 304 sample. The earlier corrosion studies on HA coatings shows the same kind of results [30–31, 40–43]. So the analysis of Tafel slope values indicates that the plasma coated HA AISI 304 specimen with lowest I_{Corr} values is the most corrosion resistant specimen among the uncoated and HA + 10 wt% CaP coated AISI 304 specimens in Ringer's solution. Singh et al. reported that the increase percentage of CaP in HA also decreases the corrosion resistance of plasma coated bio-implants [Ref 30].

The XRD peaks of HA and HA + 10 wt% CaP coated AISI 304 (Figure 5) appears more crystalline after electrochemical corrosion testing and the intensity of XRD peaks found to be increased after immersion of samples in Ringer's solution for 24 hours during corrosion testing. The sharp peaks after immersion indicates the dissolution of the amorphous phases [40]. According to Scherrer's formula average crystallite size of HA and HA + 10 wt% CaP coatings on AISI 304 after immersion in Ringer's solution are 26.46 nm and 21.88 nm respectively that reveal an increase in crystallinity after electrochemical corrosion testing. It is reported that amorphous phases are more soluble than crystalline HA as they encourage the early bone growth [44]. The dissolution was favorable for the early stages of transformation of biological equivalents that act as mediator between osteoclast and osteoblast differentiation [45]. The higher crystalline coating leads to longer implant life, while some implant manufacture prefer a faster dissolving coating to enhance the bone

growth [46]. It has been reported in in-vivo studies that the phase purity, crystallinity and microstructure of HA coatings affects the biological response of HA coating [47].

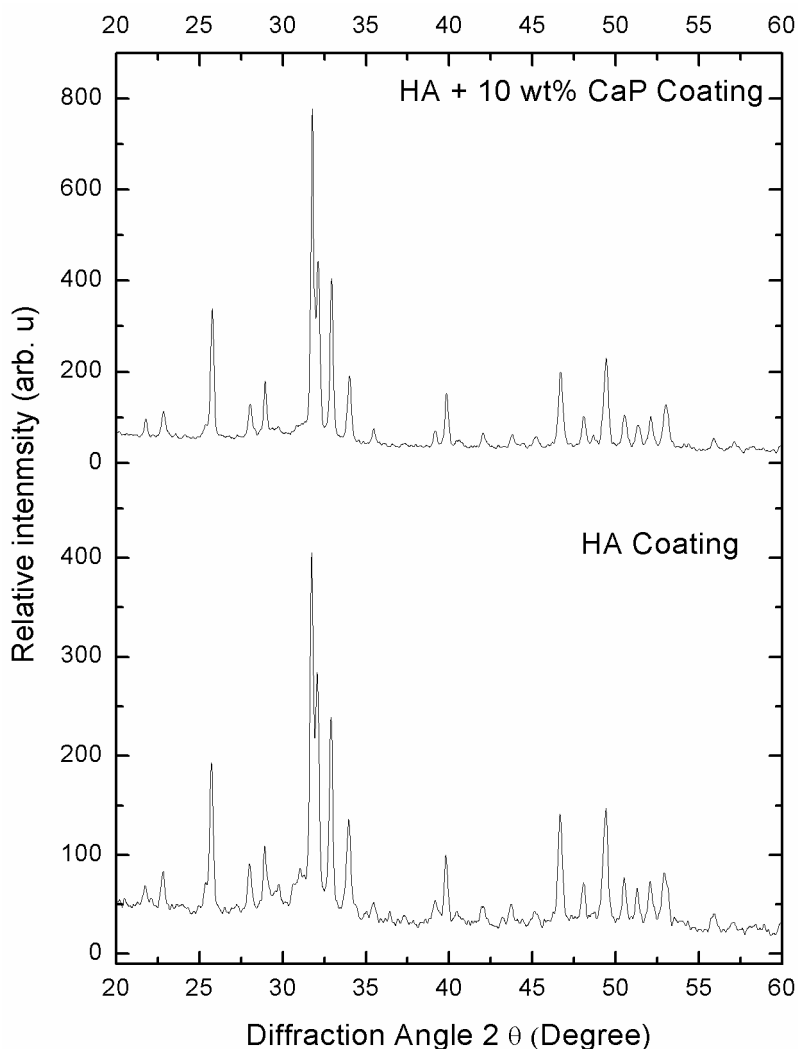


Figure 5. XRD pattern of plasma sprayed pure HA, and HA + 10 wt% CaP coating on AISI 304 after corrosion testing in Ringer's solution

After electrochemical corrosion testing, the compositional changes, if any, on the surfaces of the exposed specimens were further examined by SEM and EDX. The surface morphology of the HA coated samples (Figure 6 (a)) changes to flattened particles and looks smooth and denser after exposure to the corrosion testing in Ringer's solution. The morphology of HA + 10 wt% CaP coating (Figure 6 (b)) appears to be more porous and less smooth after 24 hour immersion in Ringer's solution for corrosion testing. The size of pores and void appear to be increased. No cracks were found on both the Ha and HA – CaP coated exposed specimens.

EDX analysis confirms the presence of Ca, P and O elements in all HA and HA + 10 wt% CaP coatings. EDX analyses of exposed specimens shows that ratio of Ca/P decreases by taking the average of elemental composition at three spectrums after 24 hour immersion in Ringer solution. The decrease in the values indicates that phosphate accumulate on the surface which suggests that incongruent dissolution of the HA has taken place [40]. No constituent of substrate i.e. Fe, Cr, Ni and Mn found on the surface of any coatings of the exposed samples.

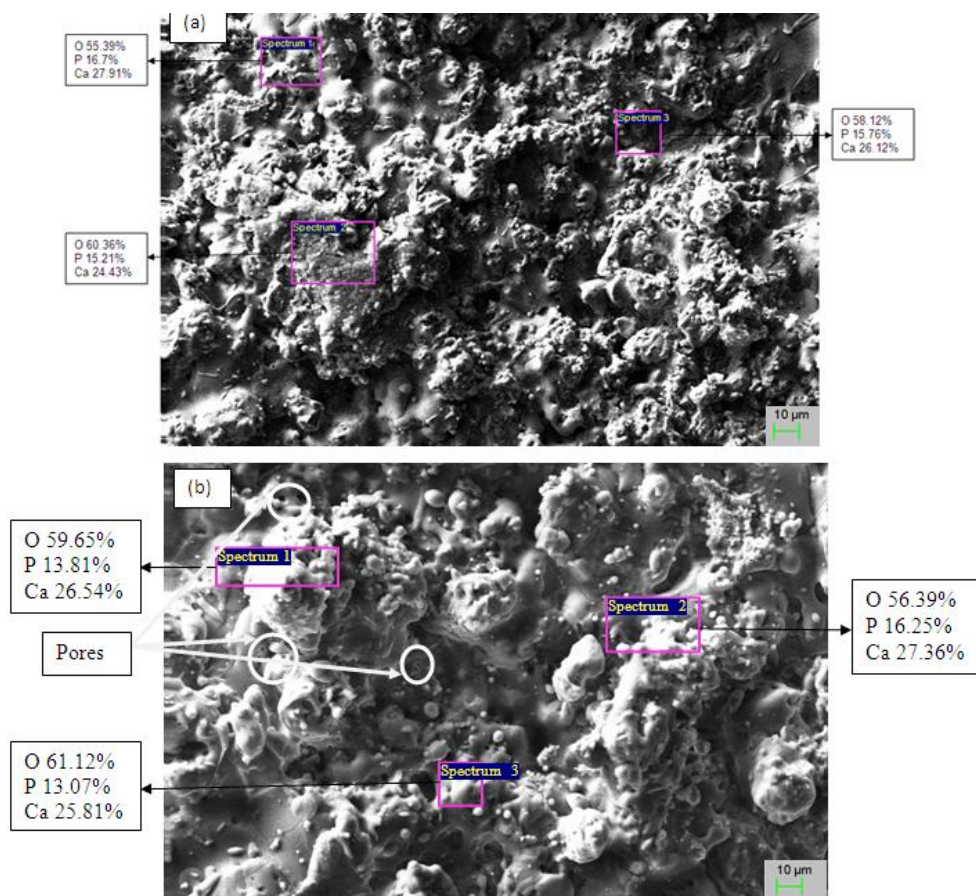


Figure 6. SEM and EDX of plasma sprayed (a) HA coating (b) HA + 10 wt% CaP coating on AISI 304 after immersion in Ringer's solution for corrosion testing

Conclusion

In the present study, plasma spray technique was used to deposit the HA and HA + 10 wt% CaP on AISI 304. The following conclusions have been drawn from the study:

1. The plasma sprayed HA + 10 wt% CaP coating is more crystalline than HA wt% CaP Coating on AISI 304.

2. The plasma sprayed HA + 10 wt% CaP coating exhibited higher surface roughness ($R_a = 7.012 \pm 0.3 \mu\text{m}$) than HA Coating on AISI 304.
3. The electrochemical study showed the corrosion resistance of the AISI 304 is more after the deposition of plasma sprayed HA than uncoated and HA + 10 wt% CaP coatings on AISI 304.

Future in-vivo studies of plasma sprayed HA and HA + 10 wt% CaP coated AISI 304 and a complete interpretation of these results can help in assessing their use in clinical applications.

References

- [1] A.C. Fraker, Corrosion, ASM Handbook, ASM International, **13**, pp1324–1335, 1992.
- [2] H. Kato, T. Nakamura, S. Nishiguchi, Y. Matsusue, M. Kobayashi, T. Miyazaki, H.M. Kim, T. Kokubo, J. Biomed. Mater. Res. **53**, pp28–35, 2000.
- [3] T. Kokubo, F. Miyaji, H.M. Kim, J. Am. Ceram. Soc. **79**, 4, pp1127–1129, 1996.
- [4] S.K. Lawrence, M. Gertrude Shults, J. Exp. Med. **42**, 4, pp565–591, 1925.
- [5] J. Ballarre, D.A. López, N. C. Rosero, A. Duran, M. Aparicio, S.M. Cere, Surf. Coat. Technol. **203**, pp80–86, 2008.
- [6] U. Kamachi Mudali, T.M. Sridhar, B. Raj, Sadhana, **28**, 3 & 4, pp601–637, 2003.
- [7] M. Lee Hee, D.W. Han, H.S. Baek, H.R. Lim, I. S. Lee, K.Y. Lee, K.T. Kim, S.J. Lee, J.C Park, Surf. Coat. Technol. **201**, pp5729–5732, 2007.
- [8] A. Balamurugan, G. Balossier, S. Kannan, S. Rajeswari, Mater. Lett. **60** (2006), 2288–2293.
- [9] T. Hanawa, J. Artif. Organs, **12**, 2, pp73–79, 2002.
- [10] H.M. Kim, F. Miyaji, T. Kokubo, T. Nakamura, J. Biomed. Mater. Res. **38**, pp121–127, 1997.
- [11] D.D Deligianni, N.D. Katsala, P.G. Koutsoukos, Y.F. Missirlis, Biomaterials, **22**, pp87–96, 2001.
- [12] L.L. Guehennec, A. Soueidan, P. Layrolle, Y. Amouriq, Dent. Mater. **23**, 7, pp844–854, 2007.
- [13] J.T. Edwards, J.B. Brunski, H.W. Higuchi, J. Biomed. Mater. Res. **36**, pp454–468, 1997.
- [14] L.L. Hench, J.M. Polak, Science **295**, pp1014–1017, 2002.
- [15] W. Paul, C.P. Sharma, J. Mater. Sci., Mater. Med. **10**, pp383–388, 1999.
- [16] U. Vijayalakshmi, A. Balamurugan, S. Rajeshwari, Trends Biomater. Artif. Organs, **18**, 2, pp101–105, 2005.

- [17] W. Weng, J.L. Baptista, *Biomaterials*, **19**, 1–3, pp125–131, 1998.
- [18] D. Shi, G. Jiang, J. Bauer, J. Biomed. Res. Appl. Biomater. **63**, 1, pp71–78, 2002.
- [19] Y. Fu, A.W. Batchelor, K.A. Khor, *Wear*, **230**, 1, pp98–102, 1999.
- [20] O.S. Yildirim, B. Aksakal, H. Celik, Y. Vangolu, A. Okur, *Med. Eng. Phys.* **27**, 3, pp221–228, 2005.
- [21] A.M. Ektessabi, M. Hamdi, *Surf. Coat. Technol.* **153**, 1, pp10–15, 2002.
- [22] H.M. Kim, *Curr. Opin. Sol. State Mat. Sci.* **7**, 4–5, pp289–299, 2003.
- [23] S. Leeuwenburgh, P. Layrolle, F. Barrere, J. Bruijn, J. Schoonman, C.A. Blitterswijk, K. Grootde, *J. Biomed. Mater. Res.* **56**, 2, pp208–215, 2001.
- [24] J. Fernandez, M. Gaona, J.M. Guilemany, *Bioceramics* **16**, *Key Eng. Mat.* **256**, pp383–386, 2004.
- [25] N. Aebli, J. Krebs, H. Stich, P. Schawalder, M. Walton, D. Schwenke, H. Gruner, B. Gasser, J.C. Theis, *J. Biomed. Mater. Res: A*, **66**, A(2), pp356–363, 2003.
- [26] J. Fernandez, J. M. Guilemany, M. Gaona, *Conference Proceedings ITSC*, E. Lugscheider, Ed., May 2–4, 2005, Basel, Switzerland (ISBN 3–87155–793–5) Ed., DVS/IIW/ASMTSS, pp1219–1224, 2005.
- [27] Y. Yang, K.H. Kim, J.L. Ong, *Biomaterials*, **26**, 3, pp327–337, 2005.
- [28] Xue W, Liu X, Zheng X, Ding C. *Surf. Coat. Technol.* **185**, pp340–345, 2004.
- [29] L. Nimb, K. Gotfredsen, J.J. Steen, *Acta Orthop. Belg.* **59**, pp 333–338, 1993.
- [30] G. Singh, H. Singh, B.S. Sidhu, *Biomimetics Biomaterials and Tissue Engineering*, **18**, 1, [doi: 10.4172/1662–100X.1000103] 2013.
- [31] G. Singh, H. Singh, B.S. Sidhu, *Applied Surface Science*, **284**, pp811–818, 2013.
- [32] FDA, Calcium phosphate (Ca–P) coating draft guidance for preparation of FDA submissions for orthopedic and dental endosseous implants. Washington, DC: Food and Drug Administration, pp1–14, 1992.
- [33] ISO, *Implants for surgery: coating for hydroxyapatite ceramics*, pp1–8, 1996.
- [34] G. Daculsi, R.Z. Legeros, E. Nery, K. Lynch, B. Kerebel, *J. Biomed. Mater. Res.* **23**, pp883–894, 1989.
- [35] W.J. Dhert, C.P. Klein, J.A. Jansen, E.A. van der Velde, R.C. Vriesde, *J. Biomed. Mater. Res.* **27**, pp127–138, 1993.
- [36] J. Delecrin, G. Daculsi, N. Passuti, B. Duquet, *Cells Mater* **4**, pp51–62, 1994.
- [37] M. Songur, H. Celikkan, F. Gokmese, S.A. Simsek, N.S. Altun, *J. Appl. Electrochem.* **39**, pp1259–1265, 2009.
- [38] B. Aksakal, M. Gavali, B. Dikici, *Mater. Eng. Perform.* **19**, pp894–899, 2010.
- [39] G. Manivasagam, D. Dhinasekaran, A. Rajamanickam, *Recent Pat. Corros. Sci.* **2**, pp40–54, 2010.
- [40] S.R. Sousa, M.A. Barbosa, *Biomaterials*, **17**, pp397–404, 1996.

- [41] G. Singh, H. Singh, B.S. Sidhu, Surf. Coat. Technol. **228**, pp242–247, 2013.
- [42] S.K. Yen, S.H. Chiou, S.J. Wu, C.C Chang, S.P. Lin, Mater. Sci. Eng. **26**, pp65–77, 2006.
- [43] S.C. Cachinho, R.N. Correia, J. Mater. Sci. Mater. Med. **19**, pp451–457, 2008.
- [44] S.H. Maxian, J.P. Zawadsky, M.G. Dunn, J. Biomed. Mater. Res. **27**, pp717–728, 1993.
- [45] W. Xue, S. Tao, X. Liu, X. Zheng, C. Ding, Biomaterials, **25**, pp415–421, 2004.
- [46] K.A. Gross, S. Saber–Samandari, J. Aust. Ceram. Soc. **43**, pp98–101, 2007.
- [47] C.Y. Yang, R.M. Lin, B.C. Wang, T.M. Lee, E. Chang, J. Biomed. Mater. Res. **37**, pp335–345, 1997.